

On collisional impurity transport in nonaxisymmetric plasmas

A Mollén¹, M Landreman², H M Smith³

¹ *Department of Applied Physics, Chalmers University of Technology, Göteborg, Sweden*

² *Institute for Research in Electronics and Applied Physics, University of Maryland, College Park, Maryland 20742, USA*

³ *Max-Planck-Institut für Plasmaphysik, 17491 Greifswald, Germany*

E-mail: albertm@chalmers.se

Abstract. The presence of impurity species in magnetic confinement fusion devices leads to radiation losses and plasma dilution. Thus it is important to analyze impurity dynamics, and search for means to control them. In stellarator plasmas the neoclassical ambipolar radial electric field often points radially inwards (referred to as the ion root regime), causing impurities to accumulate in the core. This can limit the performance of nonaxisymmetric devices.

In the present work we analyze neoclassical impurity transport in stellarator plasmas using a recently developed continuum drift-kinetic solver, the SFINCS code (the Stellarator Fokker-Planck Iterative Neoclassical Conservative Solver). The study is performed for a case close to the edge of W7-X using the standard configuration magnetic geometry. We investigate the sensitivity of impurity transport to impurity charge, main species density and temperature gradients, as well as ion temperature.

At the studied radial location we find that the neoclassical impurity peaking factor can be very large, particularly for high- Z impurities. The ambipolar radial electric field is in the ion root regime, and impurity accumulation can thus be expected. The accumulation is strengthened by the large main species density and temperature gradients. Moreover we find that the size of the bootstrap current is affected by the value of the plasma effective charge, suggesting that employing a realistic ion composition can be important when calculating the bootstrap current.

1. Introduction

The stellarator concept has an advantage over the tokamak concept, as it has the potential of steady state plasma operation with no current drive [1, 2]. However, stellarators exhibit some problems due to their inherent 3D nature. In 3D the existence of magnetic flux surfaces is not guaranteed as in axisymmetric configurations. The 3D magnetic equilibrium implies that particles can be trapped in helical magnetic wells where they can escape the plasma even in the absence of collisions. As a consequence the neoclassical transport is typically considerably larger in stellarators than in tokamaks. Furthermore, since collisionless trajectories are not necessarily confined, each species can have a different radial transport rate, resulting in a radial electric field to restore ambipolarity. This electric field is referred to as the ambipolar radial electric field, and can be determined without knowledge of the turbulent transport since the radial turbulent fluxes are automatically ambipolar to leading order in ρ_i/L , with ρ_i being the ion Larmor radius and L the smallest macroscopic scale length of interest [3].



In stellarators, the neoclassical ambipolar radial electric field often points radially inwards (referred to as the ion root regime), and this causes impurities to accumulate in the core [4–6]. This accumulation can be particularly strong for impurities of high charge Z . Since the presence of impurities leads to plasma dilution and radiation losses, where high- Z impurities are especially detrimental, it is important to study their behavior in fusion plasmas. This is an area which to date has been more extensively studied in tokamaks than in stellarators, related to the fact that the complicated stellarator geometry makes calculations demanding. In tokamak plasmas the transport is often dominated by turbulence, but since the neoclassical transport is typically much larger in stellarators it can be the main transport channel.

In the present work we perform a study of neoclassical impurity transport in stellarators using a recently developed neoclassical code SFINCS (the Stellarator Fokker-Planck Iterative Neoclassical Conservative Solver) described in [7]. This continuum code solves the 4D drift-kinetic equation, retaining coupling in four of the independent phase space variables (two spatial and two velocity), but neglecting radial coupling. The code can be used for an arbitrary number of plasma species, but in our study we will employ electrons (e), main hydrogen ions (i) and one impurity species (z).

The paper is organized as follows. In Sec. 2 we describe experimental parameters, introduce the impurity peaking factor and explain how to estimate it with SFINCS. The results are then discussed and summarized in Sec. 3.

2. Impurity density peaking

Flux-surface quantities only depend on the flux-surface label, for which we will use the normalized toroidal flux $\psi_N \equiv \psi/\psi_a$, where $2\pi\psi$ is the toroidal flux and $2\pi\psi_a$ the toroidal flux of the last closed flux-surface. This label is related to the effective radius r according to $\psi_N = (r/a)^2$, where a is the outermost effective minor radius. The density and temperature gradient scale lengths of species s are defined according to $L_{ns} = -[\partial(\ln n_s)/\partial r]^{-1}$ and $L_{Ts} = -[\partial(\ln T_s)/\partial r]^{-1}$. We now define the impurity peaking factor a/L_{nz}^0 (also referred to as the zero-flux impurity density gradient) as a/L_{nz} for which the flux-surface averaged impurity flux vanishes

$$\langle \Gamma_z \cdot \nabla r \rangle \equiv \left\langle \int d^3v f_{z1} \mathbf{v}_{dz} \cdot \nabla r \right\rangle = 0. \quad (1)$$

Here $\langle X \rangle = \left(\int_0^{2\pi} d\theta \int_0^{2\pi} d\zeta \frac{X}{B^2} \right) / \left(\int_0^{2\pi} d\theta \int_0^{2\pi} d\zeta \frac{1}{B^2} \right)$ in Boozer coordinates, $f_{z1} = f_z - f_{Mz}$ is the departure from the Maxwellian part of the distribution function, and \mathbf{v}_{dz} is the drift velocity.

The neoclassical impurity peaking factor is found with SFINCS through an iterative procedure, varying $\partial n_z/\partial r$ and the radial electric field $E_r = -\partial\Phi/\partial r$ until $\langle \Gamma_z \cdot \nabla r \rangle = 0$ and $\sum_s Z_s e \langle \Gamma_s \cdot \nabla r \rangle = 0$ simultaneously. The radial electric field for which the radial current vanishes is the ambipolar field. We will study a plasma edge scenario originally used in [8] but also considered in [7], with an extra single impurity species introduced into the hydrogen plasma. The magnetic equilibrium is the W7-X standard configuration at $r/a = 0.88$, with $n_e = 6.6 \times 10^{19} \text{ m}^{-3}$ and $T_e = T_i = 1 \text{ keV}$. The pressure gradient is large, $a/L_{ne} \approx 11.9$ and $a/L_{Te} = a/L_{Ti} \approx 5.8$, and we note that $\rho_i/L_n \approx 3 \times 10^{-2}$. The collisionality (specified on p. 10 in [7]) is below the Pfirsch-Schlüter (high collisionality) regime. As our baseline scenario we will study C^{6+} with $Z_{\text{eff}} = 1.05$, but we also analyze Ar^{18+} , Ni^{28+} and W^{40+} . The resolution used in the SFINCS runs is $N_\theta = 19$, $N_\zeta = 71$ grid points in the poloidal and toroidal direction (per identical segment of the stellarator, where W7-X has a five-fold symmetry in the toroidal direction), $N_x = 8$ grid points in energy and $N_\xi = 60$ Legendre polynomials to represent the distribution function (here $\xi = v_{\parallel}/v$), $N_L = 4$ Legendre polynomials and $N_{x,\text{Pot}} = 40$ grid points in energy to represent the Rosenbluth potentials, and $x_{\text{Max}} = 5.0$ as the maximum normalized speed for the Rosenbluth potential grid.

Figure 1 shows how the neoclassical impurity peaking factor and the ambipolar electric field vary with impurity charge, electron density gradient, ion temperature gradient, and ion temperature. We note that in the scalings where the pressure gradient is changed one should ideally generate a new magnetic equilibrium for each point to match the new pressure profile from force balance. This has however not been made due to the significant extra workload such a procedure requires; instead the baseline magnetic equilibrium is used for all the points. The transport of each plasma species in stellarators is, in general, proportional to a linear combination of the thermodynamic forces, where ZeE_r/T_z is included as a term in one of the forces of the impurity transport equation. It is thus not surprising that we find that the peaking factor is heavily dependent on the charge of the impurity, and a very strong peaking is found for high- Z impurities. The ambipolar electric field (which is in the radially inward ion root regime) is not significantly affected by changing the impurity charge, but the reason for this is that the impurity content is kept low to maintain $Z_{\text{eff}} = 1.05$ and consequently the ambipolar electric field is close to its value in a corresponding pure plasma. Furthermore we see that both the peaking factor and the strength of the radial electric field experience approximately linear increase with main species gradients. Increasing the ion (and impurity) temperature leads to an increase in the strength of the electric field, but the impurity peaking factor is reduced.

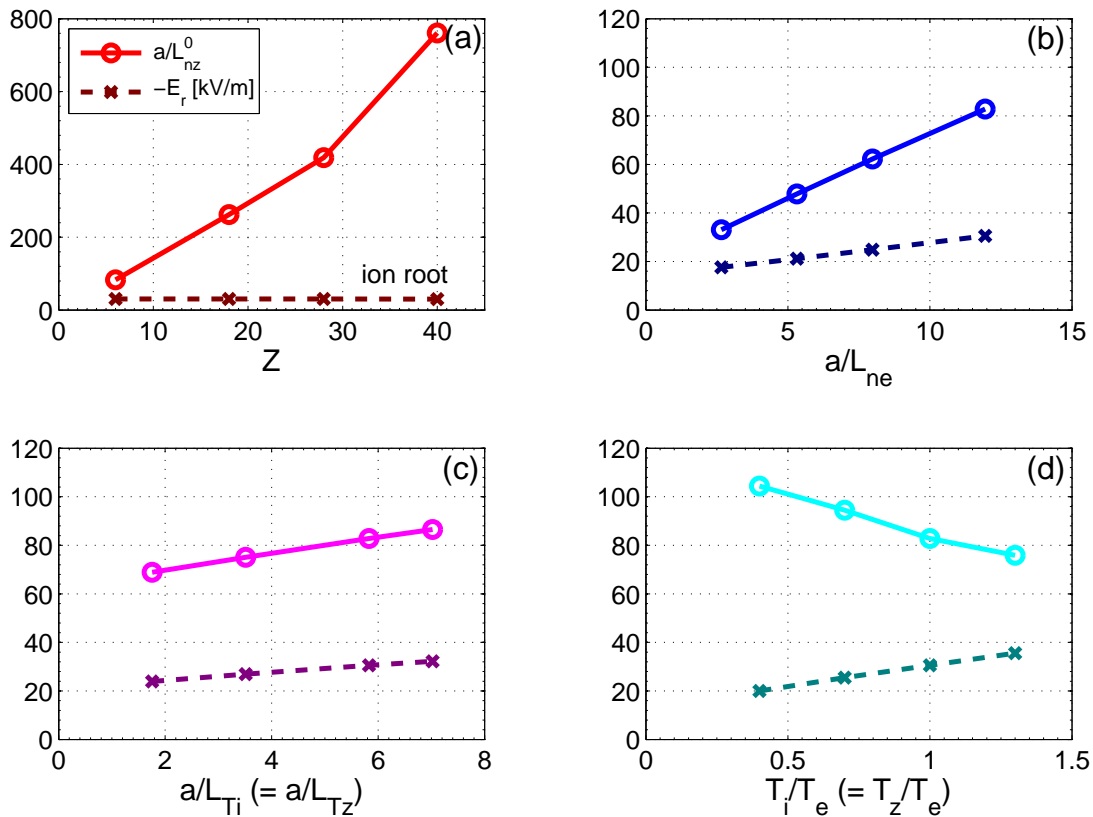


Figure 1. Impurity peaking factor (—○) and ambipolar radial electric field (---×) as functions of impurity charge (a), electron density gradient (b), ion temperature gradient (c), and ion temperature (d) with electron temperature fixed. Note that in (d) $\partial T_i/\partial r$ ($= \partial T_z/\partial r$) is fixed which implies that a/L_{Ti} ($= a/L_{Tz}$) is varying.

We can try to obtain a further insight for the results in Fig. 1 by using a simplified picture. In a typical ion root scenario, the radial electric field is approximately determined by the condition

that the radial ion flux vanishes, since the electron particle flux is typically much smaller and we look at a case when the impurity particle flux is zero. The radial ion flux is

$$\langle \Gamma_i \cdot \nabla r \rangle \propto \frac{1}{n_i} \frac{\partial n_i}{\partial r} + \frac{e}{T_i} \frac{\partial \Phi}{\partial r} + \beta \frac{1}{T_i} \frac{\partial T_i}{\partial r}, \quad (2)$$

where β is a parameter which in general depends on the radial electric field. Assuming $n_e \approx n_i$ which follows from the low impurity content, and setting Eq. (2) to zero gives an approximation to the ambipolar radial electric field

$$E_r = -\frac{\partial \Phi}{\partial r} = \frac{T_i}{ae} \left[\frac{a}{n_i} \frac{\partial n_i}{\partial r} + \beta \frac{a}{T_i} \frac{\partial T_i}{\partial r} \right] = -\frac{T_i}{ae} \left[\frac{a}{L_{ne}} + \beta \frac{a}{L_{Ti}} \right]. \quad (3)$$

Neglecting the E_r dependence in β , Equation (3) is in qualitative agreement with Figs. 1 (a)-(c), since E_r is approximately independent of Z while depending linearly (with an offset) on a/L_{ne} and a/L_{Ti} . Also Fig. 1 (d) is consistent with Eq. (3), as E_r depends linearly on T_i .

Let us now consider the impurity peaking factor. Since the peaking factor is very large and with the assumption $Z \gg 1$, in the simplest model, the only thermodynamic drive terms that matter for the impurities are $(1/n_z) (\partial n_z / \partial r)$ and $(Ze/T_z) (\partial \Phi / \partial r)$. The peaking factor is thus approximately determined from

$$0 = \langle \Gamma_z \cdot \nabla r \rangle \propto a \left[\frac{1}{n_z} \frac{\partial n_z}{\partial r} + \frac{Ze}{T_z} \frac{\partial \Phi}{\partial r} \right]. \quad (4)$$

In a more complete model, there would be other drive terms in Eq. (4) from all the other inhomogeneous terms in the system of kinetic equations. Nevertheless substituting Eq. (3) into Eq. (4) we obtain the impurity peaking factor as

$$\frac{a}{L_{nz}^0} = Z \left[\frac{a}{L_{ne}} + \beta \frac{a}{L_{Ti}} \right]. \quad (5)$$

This equation approximately reproduces the linear dependence of a/L_{nz}^0 on Z shown in Fig. 1 (a). Similarly to Eq. (3) for E_r , the linear dependence of a/L_{nz}^0 on a/L_{ne} and a/L_{Ti} is reproduced in Figs. 1 (b) and (c) with a small offset. The variation of a/L_{nz}^0 with T_i in Fig. 1 (d) is likely connected to the fact that we keep $\partial T_i / \partial r$ ($= \partial T_z / \partial r$) fixed rather than a/L_{Ti} ($= a/L_{Tz}$) when performing the scan, this implies that a/L_{Ti} is decreasing with increasing T_i/T_e .

In Fig. 2 it is shown how the main species radial flux and the bootstrap current vary with impurity charge, electron density gradient, ion temperature gradient, and ion temperature. Increasing the gradients unsurprisingly leads to a larger radially outward flux. The size of the bootstrap current is increased by increasing the ion temperature gradient, but slightly reduced by increasing the main species density gradients. Increasing the ion (and impurity) temperature leads to an increased outward flux, and has a non-monotonic effect on the bootstrap current.

Finally we investigate how the impurity peaking factor, the ambipolar radial electric field, the main species radial flux and the bootstrap current are affected by the plasma effective charge Z_{eff} . The analysis is made by changing the impurity concentration, and the results are illustrated in Fig. 3. As long as the impurity concentration is low, the main species density gradients are only weakly affected by changes in the impurity density gradient to maintain quasi-neutrality. However as the impurity content is increased the effect on the main species gradients can be considerable, and it is difficult to anticipate how they will change to keep quasi-neutrality. We therefore carry out two different scans. In the first scan we maintain radial quasi-neutrality by modifying the main ion density gradient along with the impurity density gradient. In the second scan we keep the main ion density gradient fixed as the impurity density gradient is varied,

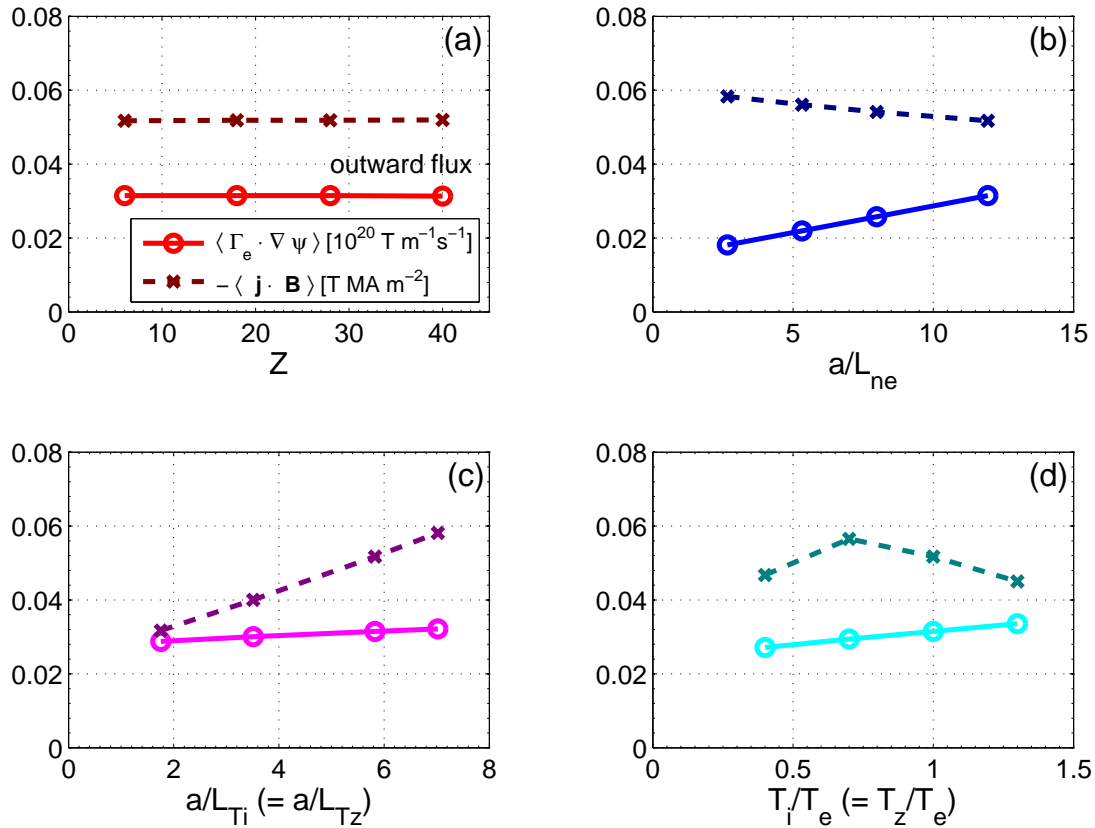


Figure 2. Main species radial flux (—○) and bootstrap current (---×) as functions of impurity charge (a), electron density gradient (b), ion temperature gradient (c), and ion temperature (d) with electron temperature fixed. Note that since $\langle \Gamma_z \cdot \nabla \psi \rangle = 0$, due to ambipolarity $\langle \Gamma_e \cdot \nabla \psi \rangle = \langle \Gamma_i \cdot \nabla \psi \rangle$, and also that in (d) $\partial T_i / \partial r (= \partial T_z / \partial r)$ is fixed which implies that $a/L_{Ti} (= a/L_{Tz})$ is varying.

violating radial quasi-neutrality. As shown in the figure, keeping the main species gradients fixed leads to an increase in impurity peaking, strength of the ambipolar electric field and main species outward radial flux with plasma effective charge, whereas the opposite trend is found when quasi-neutrality is considered. This suggests that increasing the impurity content should lead to an increase in these three quantities, but the effect is counteracted by the fact that the main species gradients are simultaneously decreased to maintain quasi-neutrality. Interestingly the size of the bootstrap current shows a similar decreasing trend with plasma effective charge in both cases, and the reduction is significant. For the case when the main species gradients are fixed there is even a sign change around $Z_{\text{eff}} = 2.15$. As the effective charge is likely to be larger than $Z_{\text{eff}} = 1.05$ in a real W7-X plasma, this could have implications on how the bootstrap current in stellarators should be calculated. Previous calculations of the bootstrap current in stellarators have almost always been made considering a pure plasma.

3. Conclusions and discussion

We used a recently developed continuum drift-kinetic solver, the SFINCS code, to study neoclassical impurity transport in stellarators. In particular, we studied a W7-X standard configuration magnetic equilibrium close to the plasma edge, considering a single impurity species

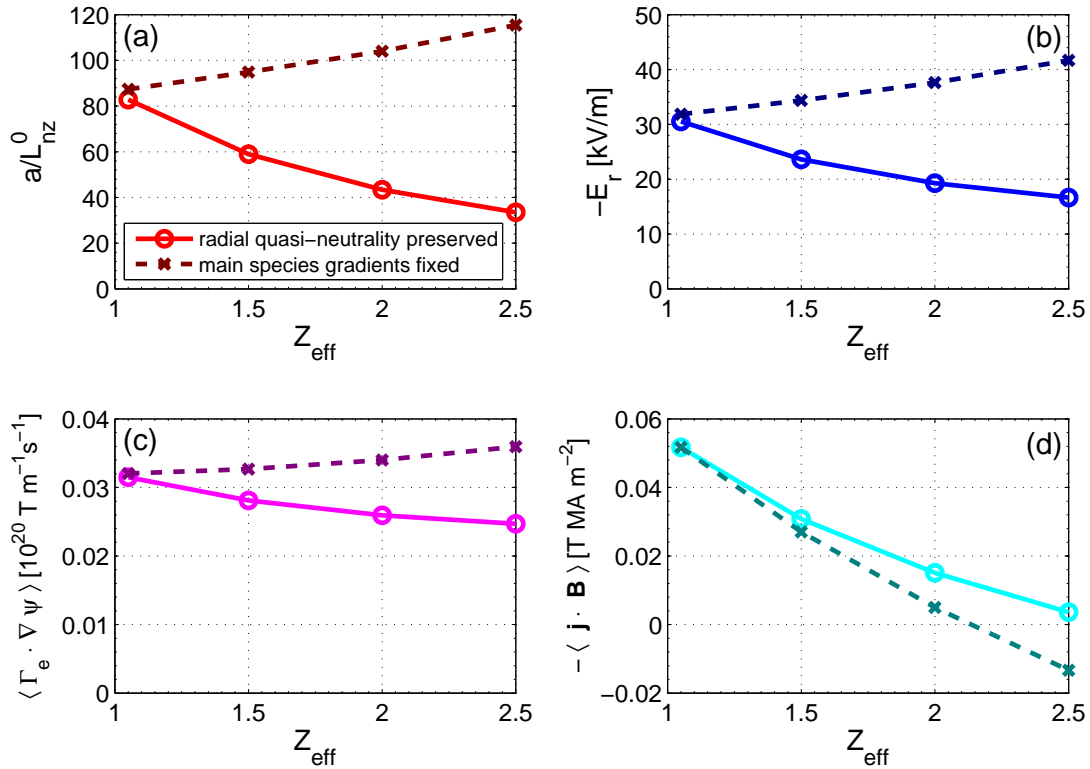


Figure 3. Impurity peaking factor (a), ambipolar radial electric field (b), main species radial flux (c), and bootstrap current (d) as functions of plasma effective charge. The analysis has been performed both maintaining radial quasi-neutrality by modifying the main ion density gradient along with the zero-flux impurity density gradient (—○), and also neglecting quasi-neutrality keeping the main species density gradients fixed (- - -×).

in a hydrogen plasma. We find that the neoclassical impurity peaking factor can be very large at the studied radial location, particularly for high- Z impurities. The peaking is amplified by the large main species density and temperature gradients. The ambipolar electric field is in the ion root regime, and it is thus not surprising to find an impurity accumulation. Furthermore we find that the bootstrap current is significantly affected by the value of the plasma effective charge. This could indicate that it is important to consider the complete ion composition when calculating the bootstrap current, rather than simply employing a pure plasma.

We note that the present analysis suggests that impurity accumulation could be a significant problem in a W7-X plasma. However we make two final remarks on the study. Firstly, in [6] it was shown that it can be important to take into account the variation of the electrostatic potential on a flux-surface, $\Phi_1 = \Phi - \langle \Phi \rangle$, since impurities are particularly affected due to their higher charge. This is not done in our analysis and would require implementing extra terms in the kinetic equation solved by SFINCS. Secondly, since we calculate the neoclassical impurity peaking the contribution from turbulence to the impurity transport is completely neglected. Turbulence in stellarators is an area where much remains to be explored [2]. It is thus difficult to tell if the turbulent impurity transport would contribute significantly or possibly even dominate over the collisional impurity transport. In tokamak plasmas the impurity peaking can in many cases be determined almost solely by the turbulent transport, since the collisional transport is typically much lower than the turbulent transport, in contrast to stellarators. The

impurity peaking factors found from a gyrokinetic approach in tokamaks are much smaller than the peaking factors presented in this work, typically $a/L_{nz}^0 \sim \mathcal{O}(1)$. It is therefore not unlikely that turbulence could cause a reduction of the large impurity peaking we find here. The neoclassical pinch velocity of the baseline case in our study is estimated to be $V \sim 0.2 v_{Ti} (\rho_i/a)^2$ (corresponding to 0.2 in gyro-Bohm units), which is of the same order as a typical turbulent impurity pinch in tokamaks.

Acknowledgments

The authors are grateful to J Geiger for providing the W7-X equilibrium data, and to I Pusztai, T Fülöp, C D Beidler and P Helander for input on the work. This project has received funding from the European Union's Horizon 2020 research and innovation programme under grant agreement number 633053. The views and opinions expressed herein do not necessarily reflect those of the European Commission.

References

- [1] Kikuchi M, Lackner K and Tran M Q 2012 *Fusion physics* (Vienna: International Atomic Energy Agency)
- [2] Helander P et al 2012 *Plasma Phys. Control. Fusion* **54** 124009
- [3] Helander P 2014 *Rep. Prog. Phys.* **77** 087001
- [4] Braun S and Helander P 2010 *Phys. Plasmas* **17** 072514
- [5] Braun S 2010 Effect of Impurities on Kinetic Transport Processes in Fusion Plasmas, PhD thesis Max-Planck-Institut für Plasmaphysik <http://ub-ed.ub.uni-greifswald.de/opus/volltexte/2010/888/>
- [6] García-Regaña J M, Kleiber R, Beidler C D, Turkin Y, Maaßberg H and Helander P 2013 *Plasma Phys. Control. Fusion* **55** 074008
- [7] Landreman M, Smith H M, Mollén A and Helander P 2014 *Phys. Plasmas* **21** 042503
- [8] Turkin Y, Beidler C D, Maaßberg H, Murakami S, Tribaldos V and Wakasa A 2011 *Phys. Plasmas* **18** 022505